Scientific Research Publishing

International Journal of Geosciences, 2024, 15, 605-631
https://www.scirp.org/journal/ijg
ISSN Online: 2156-8367
ISSN Print: 2156-8359

# Mapping of Flood Risk Zones Using Multi-Criteria Approach and Radar: A Case Study of Ala and Akure-Ofosu Communities, Ondo State, Nigeria

**Olamiposi Caleb Fagunloye**

Department of Remote Sensing and Geoscience Information Systems, Federal University of Technology, Akure, Nigeria
Email: calebkolade@gmail.com

**How to cite this paper:** Fagunloye, O.C. (2024) Mapping of Flood Risk Zones Using Multi-Criteria Approach and Radar: A Case Study of Ala and Akure-Ofosu Communities, Ondo State, Nigeria. *International Journal of Geosciences*, **15**, 605-631.
https://doi.org/10.4236/ijg.2024.158035

**Received:** November 28, 2023
**Accepted:** August 26, 2024
**Published:** August 29, 2024



## Abstract

Floods are among the worst natural catastrophes, devastating homes, businesses, public buildings, farms, and crops. Studies show that it's not the flood itself that's deadly but people's vulnerability. This study investigates the Ala and Akure-Ofosu flood-prone zones; identifies elements that cause flooding in the study area; classifies each criterion by its effect; develops a flood risk map; estimates flood damage using Sentinel-1A SAR data; compares AHP results. Literature study and GIS-computer database georeferenced fieldwork data. Photos from the 2020 Sentinel 2A satellite have been organized. Built-up area, cropland, rock, the body of water, and forest Land use and cover, slope, rainfall, soil, Euclidean River Distance, and flow accumulation were mapped. These variables were integrated into a Multi-Criteria Analysis (MCA) using GIS tools, resulting in the creation of a flood risk map that categorizes the region into five risk zones: 5% of the area is identified as high-risk, 21% as low-risk, and 74% as moderate-risk. Copernicus SAR data from before and after the flood were processed on Google Earth Engine to map flood extent and ensured that the MCA map accurately reflected flood-prone areas. Periodic review, real-time flood susceptibility monitoring, early warning, and quick damage assessment are suggested to avoid flood danger and other environmental problems.

## Keywords

Remote Sensing, Flooding, GIS, Akure, Flood Risk, Damage Assessment

## 1. Introduction

Floods are a natural occurrence that is capable of occurring in practically any place

and do so regularly. A flood can be broken down into its most fundamental component: the buildup of water over ordinarily dry areas. In our globe and our communities, flooding is an inevitable and natural occurrence. The only time it poses a threat is when it comes into contact with the built environment. Floods are a natural occurrence that is capable of occurring in practically any place and do so regularly. A flood can be broken down into its most fundamental component, which is the buildup of water over ordinarily dry areas. In our globe and our communities, flooding is an inevitable and natural occurrence. The only time it poses a threat is when it comes into contact with the built environment. Floods are often regarded as the most destructive type of natural calamity that can occur and are responsible for more than 30 percent of the total damage caused by all-natural calamities, including the destruction of land, buildings, and infrastructure facilities across the world. In recent years, it has become one of the natural disasters that occur with the greatest frequency [1]. Many people believe that flooding is the natural hazard that poses the greatest risk to human life and occurs the most frequently around the world. In recent years, natural disasters, particularly floods, have had a devastating effect on society as a whole, as well as on long-term sustainable development. The ever-increasing impacts of climate change, which have been exacerbated by extreme weather events like floods and droughts, have left an indelible mark on the lives of a great number of people as well as the natural world. Over the course of many years and in virtually every region of the world, extreme rainfall brought on by climate change has led to flooding, which has been responsible for the loss of both lives and property. Many nations' efforts to advance their economies have been put on hold as a result of the unpleasant experiences they have faced. More lives and properties are becoming susceptible to the risk of flood hazards whenever catastrophic storms take place since the global population is increasing at an alarming rate, and there has also been an increase in the development of infrastructure over the past several decades [2] [3].

A flood risk assessment identifies flood mitigation measures and recommends what to do before and during a flood. Total risk is the predicted number of lives lost, people hurt, property damage, and economic disruption due to a natural phenomenon. It is the result of items at risk and specific risk [4]. Risk (total) = Hazard * Risk Elements * Vulnerability" [4].

Vulnerability, exposure, and Hazard are popular terms.

Vulnerability is the risk of physical harm. Flooding threatens the economy, infrastructure, and lives. Land cover and land use, population (age, health, mobility), built-up regions and building type, and the ability to foresee and strategize affect flood susceptibility [5]. This means that while exposure and flood risk may be the same in a given flood danger region, vulnerability may vary dependent on the listed criteria. [6] describes flood vulnerability as physical, economic, infrastructure, and social. According to the World Risk Report [7], natural catastrophes affect countries differently. Different factors affect vulnerability, as mentioned above. Nigeria, ranked 25th, has a natural catastrophe risk index of 13.09.

When people and their livelihoods, as well as natural services and resources, infrastructure, and economic, social, and cultural assets, are in danger because they are not adequately safeguarded, this is called exposure [8]. Dynamic nature of susceptibility and exposure. These two variables are affected by environmental, social, economic, topographical, demographic, ethnic, and governmental influences throughout time and space.

According to the World Meteorological Organization's Atlas of Mortality and Economic Losses from Weather, Climate, and Water Extremes (1970-2019), there were over 11,000 documented disasters worldwide linked to these hazards, resulting in slightly more than 2 million deaths and US$3,640,000,000,000 in damages [9]. EM-global DAT's disaster databases were analyzed [2]. The UN forecasts a 35% rise in flood economic hazards due to rising exposure and economic assets [10].

Heavy rainstorms and ocean storms near the coast are natural sources of flooding, whereas ruptured water main pipes, poor drainage, dam collapse, and spills are artificial causes. Coastal, river, flash, and urban flooding are regular occurrences in Nigeria. In recent decades, numerous states and cities experienced unprecedented and disastrous floods, undermining the government's capacity to avert such catastrophes. Devastating food events in Nigeria date back to 1963 in Ibadan, when the Ogunpa River overflowed, causing loss of lives and property; these hazardous events reoccurred in 1978, 1980, and 2011, with estimated damages and deaths of over 30 billion Naira and 100 people respectively, making Ogunpa River nationally and internationally famous [11] [12].

However, to implement a complete and comprehensive approach to assessing the risk of flooding, it appears that a thorough grasp of the processes of hazard, vulnerability, and risk perception is important. The major purpose of this study is to provide clarification on these concepts and to highlight a technique for the evaluation of flood hazards and flood risk.

In the process of evaluating and managing flood risks, the use of geographic information systems (GIS) and remote sensing has shown to be extremely helpful and beneficial. The real-time monitoring of flood disasters, early warning systems, and quick damage assessments have all seen significant improvements as a result of advancements in remote sensing technologies and Geographic Information Systems (GIS). Remote sensing is the science, technology, and art of gathering data about an object or region without having any physical contact with such an object [13]. It gathers data quickly across broad areas. Remotely sensed pictures can be used to map flood plains, land use, flood detection and forecasting, rainfall mapping, evacuation planning, and damage assessment. Remote sensing data, such as satellite images, provides a vast synoptic overview that may be utilized for a variety of applications. One of these applications is the mapping of the variability of terrain features, which is required for flood analysis [13]. The Geographic Information System (GIS) is a computer-based system that provides the capability for inputting, maintaining, analyzing, and modifying the massive amounts of data

acquired for flood risk assessment and management. GIS provides several methods for modeling flood-affected regions and identifying flood-prone locations. Remote sensing and GIS have become essential for monitoring floods. GIS and remotely sensed data may be utilized in phase one of flood disaster management to warn and monitor natural catastrophes and build disaster risk maps. In phase two of flood disaster management, remotely sensed data and GIS may be utilized to evaluate damage and guide relief and rescue activities in difficult-to-navigate locations.

The Ala River floodplain is most in danger. This was evident during the fieldwork in the research region. Human behavior is the primary reason why this region often experiences floods. Deforestation and improper sewerage system are the primary causes of environmental degradation in the reserves, along with clogged drains and crumbling roads.

This work is a significant addition to mitigating flood effects in Ala Basin Communities since it will inform flood risk management and spatial planning in the municipality.

## 2. Study Area

The Ala River basin includes Akure Ofosu and Ala River. Akure Ofosu lies between 6˚57'46.8"N and 5˚21'14.4"E, while Ala is 7˚17'45.6"N and 5˚1'48"E. Akure-Ofosu is 392.38 $Km^2$ and Ala is 192.80 $Km^2$, making the study area 585.18 $Km^2$. The research was conducted in the region under the jurisdiction of Akure South Local Government. According to the Koppen climate classification system, this region has an AF climate, which is defined by a brief dry season and an annual rainfall of at least 60 mm [14]. Several different types of topographic features, including spurs, saddles, valleys, and river channels, may be found in the studied region from a geomorphological perspective. The Ala River, which begins in the northwest of Akure city and runs southeast through Oba-Ile and into Edo State, has a total length of approximately 57 kilometers but is only about 14.8 kilometers long inside Akure Township [15]. However, tectonic activity and other types of disturbance have caused fracturing, jointing, and cracking in these Precambrian rocks [16] [17]. In terms of geology, the area is a component of the basement complex that is found in the southwestern region of Nigeria [16] [18]. Chanockite, Migmatite gneiss, Quartzite, and Biotite gneiss are the predominant kinds of rocks in the region, and the area receives an average rainfall of 2378 millimeters. **Figure 1** shows a map of the study area.

## 3. Materials and Methods

This chapter discusses the strategy and tools that were used to analyze the research region, including the main and secondary data and the programs that were put to use. The methods used to properly analyze data and draw conclusions are summarized here.

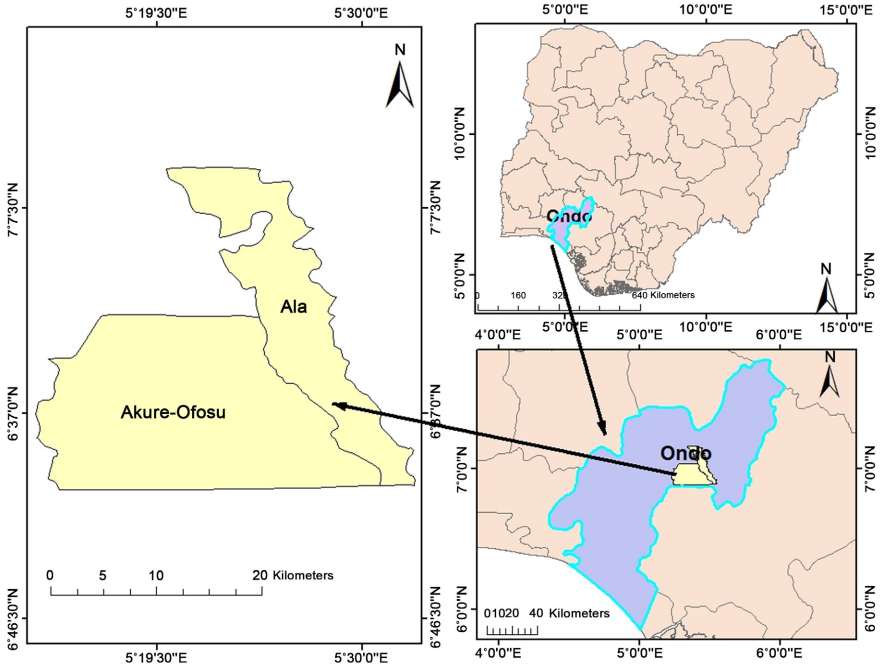


Figure 1. Map showing Ala and Akure-Ofosu communities (Communities within the Ala Basin), Ondo State, Nigeria.

### 3.1. Remote Sensing Data

The Ministry of Lands and Forestry and the Ministry of water resources works, and housing do not have geospatial data on land use and land cover, average river water levels above mean sea level, etcetera. Even satellites held by the government (Nigeria SAT 1 and 2) at the time of the investigation are not open source. Private companies having geographical data sell them. This study uses open and free data, including Sentinel 1A SAR imagery, Sentinel 2 satellite imagery, and the Shuttle Radar Topography Mission (SRTM) version 3, a product of NASA and NGA (Table 1).

- Sentinel 1A;
- Sentinel 2;
- NASA SRTM DEM;
- Rainfall Data;
- Soil Map of Nigeria.

Table 1. The data used and their sources.

| Data | Attributes | Source | Data Type | Year of Acquisition | Access |
|---|---|---|---|---|---|
| SRTM (Version 3) | Elevation, Slope, Flow Accumulation, River Distance | United State Geological Survey Earth Explorer (USGS - EE) | Raster | 2013 | Public/free to use |
| Sentinel 1A SAR-data | Flooded Area | European Space Agency | Radar | 2020 | Public/free to use |
| Sentinel 2A | Land use and Land Cover | European Space Agency | Raster | 2021 | Public/free to use |

**Continued**

| | | | | | |
|---|---|---|---|---|---|
| Original Geology (soil type) | Soil type | FAO Soil Data | Vector | | Public/free to use |
| Geology (soil type) | Soil type | Generated by Author | polygon | | Public/free to use |
| Rainfall (precipitation) | Amount of Rainfall | Tropical Rainfall Measuring Mission | word | 2021 | Public/free to use |
| Boundary | Study Area | GRID3.org | Vector | | Public/free to use |
| Farm boundary | | https://bit.ly/3TsU0je | Vector | 2021 | Public/free to use |

### 3.2. Software Used

- ArcMap 10.5;
- Microsoft Excel (2019);
- Google Earth Pro;
- Google Earth Engine (Online Platform).

### 3.3. Methods

The work's technique is dependent on the correctness of the analysis of the satellite picture (which is also dependent on preprocessing). The goal of this thesis is to use remote sensing data in ArcMap to create a flood danger map for the settlements of Ala and Akure-Ofosu. A survey of the research region was carried out to identify the factors that may be responsible for floods (like deforestation, River encroachment, and drainage blockage). Flow Accumulation (Drainage/stream network), Elevation, Slope, Land Use/Cover, Geology (soil type), and Rainfall Intensity were judged to have such an impact (precipitation).

Multi-Criteria Analysis (MCA) is used to identify flood-prone locations [19]. A two-step process is used to analyze the MCA. In the first step, the weights of the criteria are determined using Analytic Hierarchy Process (AHP), a multi-criteria decision technique. AHP creates a decision criteria hierarchy by comparing each pair of criteria in a matrixed form [20]. The weighted scores generated by the paired comparisons show the relative relevance of certain factors. To create the flood danger map, a weighted overlay procedure is used in the second step once the weights have been calculated. Synthetic Aperture Radar from Sentinel 1 was processed on Google Earth Engine (Web Platform) using the step-by-step guide provided by the United Nations Office of the Outer Space Affairs UN-SPIDER Knowledge Portal. The results from the MCA and Radar analysis were superimposed on one another to verify the accuracy of the MCA approach and to measure the flood extent in both analyses. The methodology's flow chart is shown in **Figure 2**.

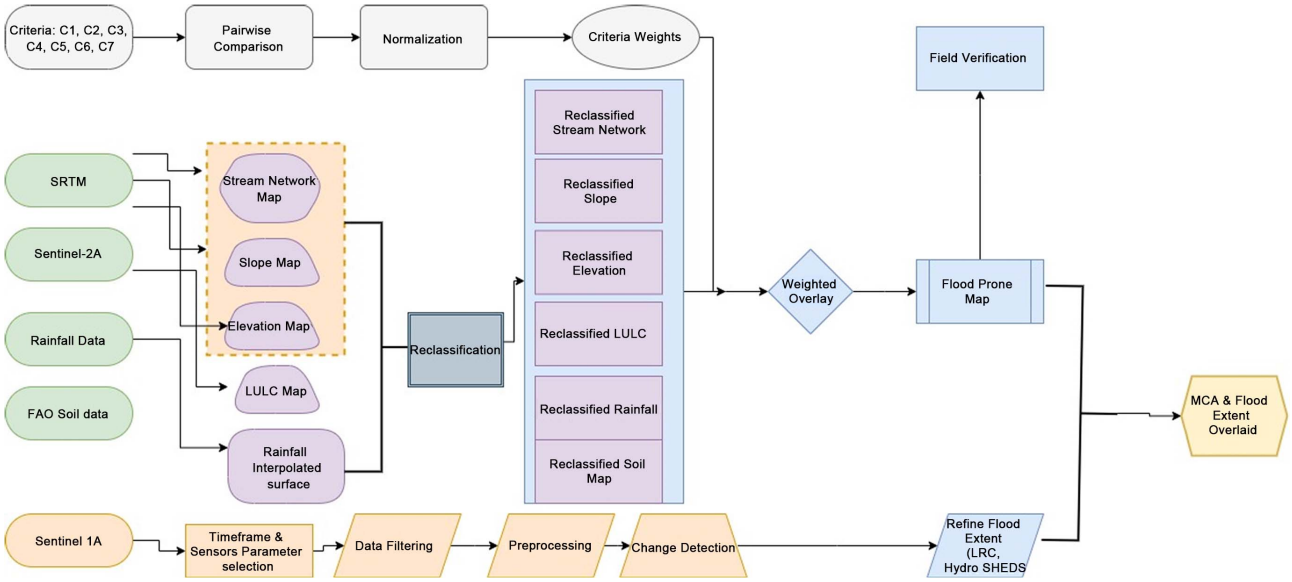


**Figure 2.** Details of the methodological framework.

### 3.3.1. Accuracy Assessment

This refers to a method of assessing the quality of categorized images [13]. The major purpose of this procedure is to verify the accuracy of the categorization process. Unsupervised classification results, class definitions, and ground truth data were all used to assess this study's accuracy. Images from Google Earth were used to compare the categorized image's reference points. Each image utilized in the research was subjected to an accuracy evaluation. There are two types of accuracy, according to [13]. User's and Producer's accuracy types. The former is comparable to a Commission error (inclusion). Images were evaluated using error matrices, which indicate a comparison of the reference values and the values assigned, and accuracy totals in percentages based on the findings in the confusion error matrix.

Kappa statistics, which show how close the agreement was and how close it would have been by chance, were also calculated. For instance, if the Kappa (k) value is 0.85, this indicates that there is 85% more agreement than would be predicted by random chance [21].

### 3.3.2. Flood Vulnerability

A map depicting the danger of flooding was produced by superimposing reclassified information based on the type of land use and land cover, the Digital Elevation Model (DEM), flow direction, flow accumulation, the type of soil, and the geographical distribution of rainfall. The kind of land use or land cover cannot be utilized on its own to estimate flood risk since the surface features are determined by the elements that were just discussed. In varying degrees, each of these elements may increase or decrease the likelihood that a certain region would be flooded. ArcMap's built-in image analysis capabilities were used to transform many datasets into raster formats for easier viewing. After that, they were recategorized using the Spatial Analyst Tool, and values were given using a rating scale that

ranged from 1 to 5 depending on how much of an effect each factor had on human susceptibility, surface water flow, and water infiltration.

The rating assigned the value "5" to locations with a very high risk, while the value "1" was given to locations with low risk. After this, each of the layers from the various datasets was given a weight based on its significance in causing or leading to flooding, overland flow, and water percolation after precipitation events, and then they were layered on top of one another to produce a flood risk map. The weights were determined based on the influence that each of the layers had on the risk that was posed to humans.

## 4. Results

Using several variables, including rainfall, soil type, elevation, land use/land cover, slope, flow direction, and flow accumulation, a study has been conducted on the locations in Ala and Akure-Ofosu communities that are in danger of flooding. Tables, maps, graphs, and charts are used to display the findings.

### 4.1. Sentinel 2A Image Processing

#### 4.1.1. Image Preprocessing

Band combination was one of the steps of the preprocessing method that was performed on the images (band combination 3, 2, 1). This allowed for a variety of band combinations to be used throughout the image classification process, which ultimately led to the greater ease with which images could be read.

#### 4.1.2. Classification of Images

**Figure 3** illustrates the findings that were obtained by the supervised classification. Bands RGB-5:43 were utilized to create false composite images that were employed in the feature identification process. The significance of band 4 and band 3 in distinguishing between different types of vegetation and in determining where the land ends and the water begins led to the selection of these combinations. After supervised classification, map features were categorized into 5 classes. The classes are described below.

#### 4.1.3. Land Use/land Cover Extent of Study Area

The study area has an estimated land area of 585.19 $km^2$ (58519.017 hectares). Supervised classification is done here, the classes of features in the study area are divided into five (5) classes which are: Built-up, Rock, Cropland, Forest, and Water body as shown in **Figure 4**. From the supervised classification, the Water body covers about 54.53 $km^2$, Built-up covers about 130.95 $km^2$, Cropland covers about 116.63 $km^2$, Rock covers about 74.92 $km^2$, and Forest covers about 208.73 $km^2$.

According to the chart in **Figure 3**, as long as illegal and unchecked deforestation continues, the built-up area will quickly rise above the crops and press in on the Forest. When built-up areas have impermeable surfaces, infiltration is decreased. The pattern of land use/land cover is very important in the evaluation of floods. The type of land cover in a location has an effect on the quantity of infiltration and percolation that occurs in that area.

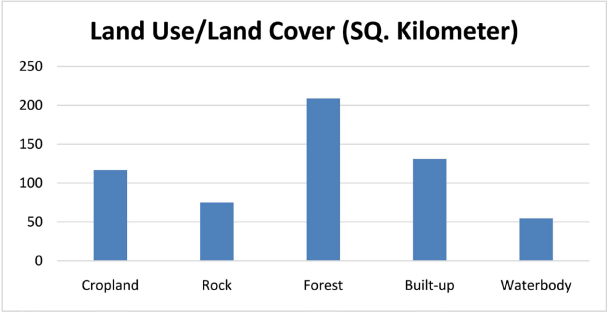


Figure 3. Land use and land cover extent of the study area.

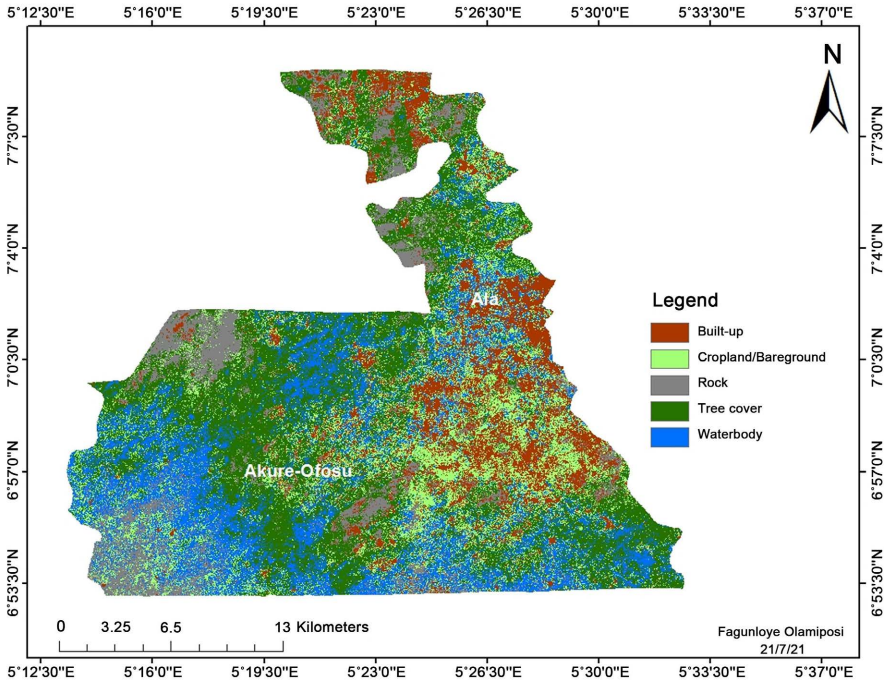


Figure 4. Supervised classification of the study area.

## 4.2. Flood Vulnerability

When generating a flood risk map, a variety of criteria were considered. Different physical criteria were used to assess vulnerability for this research, including land use/cover characteristics, geology (Soil type), topography (slope angles), hydrology (Euclidean River Distance and Flow Accumulation), and rainfall (spatial distribution). A flood risk map for the research region was created by incorporating all the aforementioned elements.

### 4.2.1. Flood Vulnerability Zoning, Based on the Land Cover Distribution

The different types of land cover must be carefully considered when assessing flood risk. Land cover affects land use and soil stability through infiltration and erosion. Less vegetation increases surface runoff. Forested and scrubland regions reduce rainwater runoff. Impermeable surfaces like concrete, roads, and buildings restrict water's capacity to percolate into the soil and increase surface runoff.

LULC features are crucial for measuring a region's flood risk vulnerability.

The class distribution illustrates the many different ways that land cover and land use may change throughout time. There was a total of five classes produced. These included a bare surface, a body of water, vegetation, and built-up areas. After that, the classes were reorganized into five distinct classes according to the impact that each factor had on the likelihood of flooding and the degree to which people were put in danger as shown in Figure 5. It is more likely to find habitation in areas that are classified as settlements, while it is less likely to find inhabitants in regions that are classified as wetlands. In many situations, the built drainage lines and culverts in metropolitan areas are frequently too narrow to accept stormwater. As a result, during precipitation events, water overflows onto the roads and pavements. The issue is made much worse by the massive volumes of solid waste that are improperly disposed of and clog the drainage systems. Therefore, land cover characteristics and land use activities only add to the flood risk that is already posed by the infiltration capacity of the soil, the nature of the slope on which land use activities are carried out, or the geology of the areas that fall under each LULC category because it influences the drainage system. The risk of flooding in a region is increased when both the land's usage and its cover are modified; in particular, when vegetation is cleared away.

Built-ups have the lowest soil infiltration capacities and are highly DE-vegetated. Paved roads and enhanced drainage provide impermeable surfaces in these places. Vegetation removal to develop residential areas and farmland changes soil structure. The water body ranked lowest because it often floods and is uninhabitable unless reclaimed. Forests may delay and reduce peak floodwater flows at local levels, but scientific data shows they cannot avoid catastrophic large-scale floods, which are typically blamed on forest removal or conversion to agricultural uses. Forest was second-to-last.

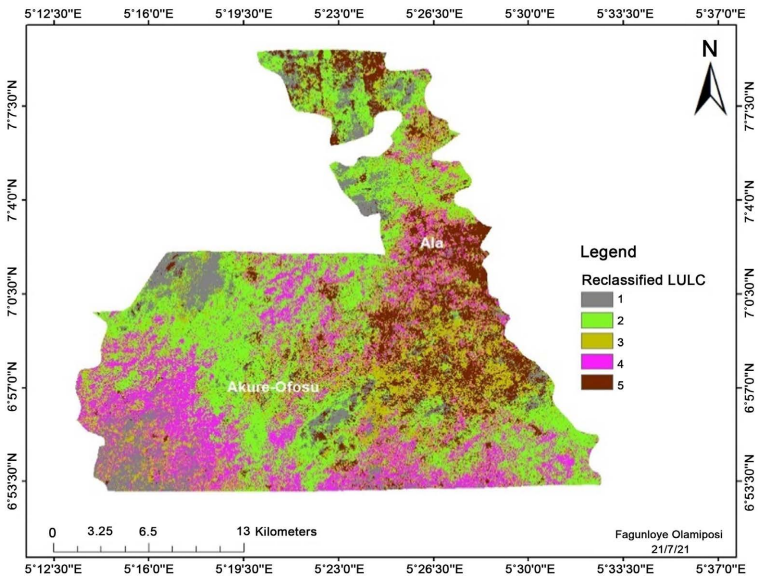


Figure 5. Reclassified land use and land cover map.

### 4.2.2. Land Cover Classification Accuracy Assessment

An error matrix is used to evaluate the supervised classification's accuracy. Error matrix values are derived by comparing feature classes given to features during classification with the feature's actual value from satellite imagery, which is used in error analysis (Google earth). Points created at random are used in this process. Each class had a minimum of fifty (50) randomly selected locations in the research region (Figure 6). To determine the value of each point, Google Earth was used. The categorized picture also identifies the value of these three hundred random dots. When these two values are compared, the erroneous features are identified and listed in the error matrix table. The comparison resulted in the creation of an error matrix table (Table 2).

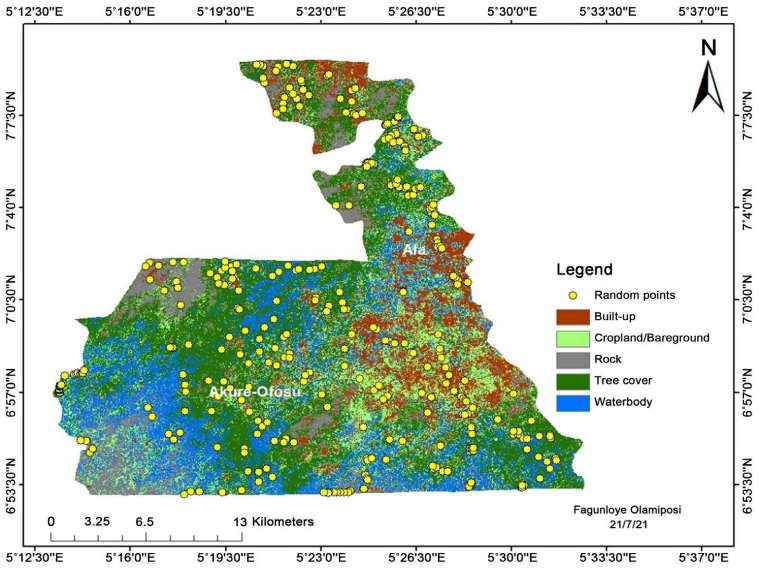


Figure 6. Random points.

Table 2. Table of error matrix.

| | water | urban | Forest | vegetation | bare ground | total row |
|---|---|---|---|---|---|---|
| **waterbody** | 43 | 0 | 2 | 3 | 2 | **50** |
| **Built-up** | 0 | 62 | 1 | 2 | 5 | **70** |
| **Forest** | 2 | 1 | 53 | 4 | 0 | **60** |
| **cropland** | 0 | 1 | 2 | 56 | 1 | **60** |
| **Rock** | 0 | 2 | 2 | 1 | 55 | **60** |
| **total column** | **45** | **66** | **60** | **66** | **63** | **300** |

Sum of diagonal = 269

Overall accuracy = (269/300)*100 = 89.7%

| **Producer accuracy** | | **User accuracy** | |
|---|---|---|---|
| Waterbody | 96% | Waterbody | 86% |
| Built-up | 94% | Built-up | 89% |

| | | | |
|---|---|---|---|
| Forest | 88% | Forest | 88% |
| Cropland | 84.8% | Cropland | 93.3% |
| Rock | 87.3% | Rock | 91.7% |

$$\text{Kappa coefficient} = \frac{300(269) - 18210}{3002 - 18210} = 87\%$$

#### 4.2.3. Flood Vulnerability Zones Based on Elevation and Slope Angles

The research region has a variety of slopes, ranging from low to medium to high. This study's slope map was created using SRTM version 3 data (void-free DEM). Because their inclinations aren't as extreme, the slope classes with lower values received higher placements. For floods, classes with the greatest slope values were ranked lower. The buildup of water in these locations does not lead to floods. Areas with limited infiltration capabilities and poor drainage, such as clay or clay loam (as shown in the study region), little vegetation, and land use activities that impede percolation, such as settlements, pose the highest flood risk (**Figure 7**).

The slope is one of the most important criteria considered when analyzing the area's flood risk. The steeper the slope angles in a region, the closer they are to the sea level. Consequently, places located at the lowest point of the elevation have the largest probability of flooding in the case of precipitation. The findings imply a slope with gentle undulations. The bulk of the region consists of flat terrain with slopes of ≤ 1.25˚, which was rated "extremely high" in the evaluation of flood risk factors. The least angle is occupied by the steep hills. The slope range between 10 and 16 degrees is considered moderately steep. It will take some time for runoff to collect to levels that may be regarded to represent a flood danger in these regions. Stormwater travels at a reasonably rapid rate and provides minimal danger of flooding as a result. Above 16 degrees, water travels at a reasonably rapid rate; hence, these locations are not susceptible to floods.

Areas between 16˚ and 47˚ are deemed to have a high runoff, to be of low relevance, and to be less susceptible to our research interests. Slope and elevation have a key impact on the stability of the ground [22].

#### 4.2.4. Flood Vulnerability Zones Based on Soil

In this research, the classification of soils was based on type (**Figure 8**). The soils in the research regions were classified as sandy clay loam and sandy loam. The soil type with the potential to create high flood rates was awarded the rank "4", while the soil type with the lowest possibility of creating a flood was allocated the rank "1." The texture of the soil has a significant effect on floods. Due to their big soil particles, sandy soils enable water to move through them quicker than other soil types, resulting in less runoff. Compared to other soil types, clay soils contain small particles, are less permeable, and enable runoff to accumulate over a longer period. This implies that places with clay soil are more susceptible to and likely to be damaged by floods. In examining the influence of soil type on floods, soil structure and infiltration capacity are also significant considerations. These aid in assessing the absorption capacity of the soil.

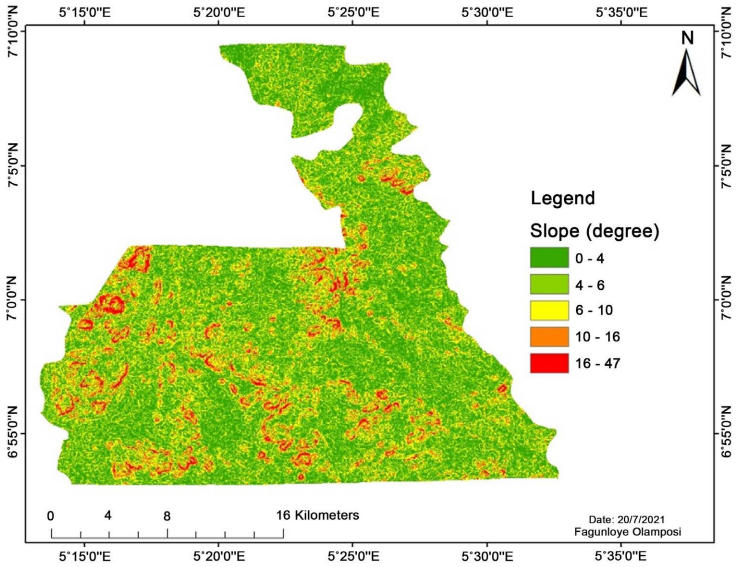


**Figure 7.** Slope map.

Different kinds of soil have varying infiltration capabilities. As a result of increased surface runoff, locations with soil that have a high infiltration capacity are susceptible to flooding. When runoff accumulates at a pace greater than the soil's capacity for percolation or infiltration, flooding occurs.

### 4.2.5. Flood Vulnerability Zones Based on Spatial Rainfall Distribution

Rainfall patterns were generated using yearly rainfall data and based on the average annual rainfall for the area. The average yearly rainfall for 2017 was utilized in this calculation. The data had previously been interpolated using the Inverse Distance Weighting (IDW) method and was in the form of a continuous raster encompassing the region of research. Five groups were derived from the data. It

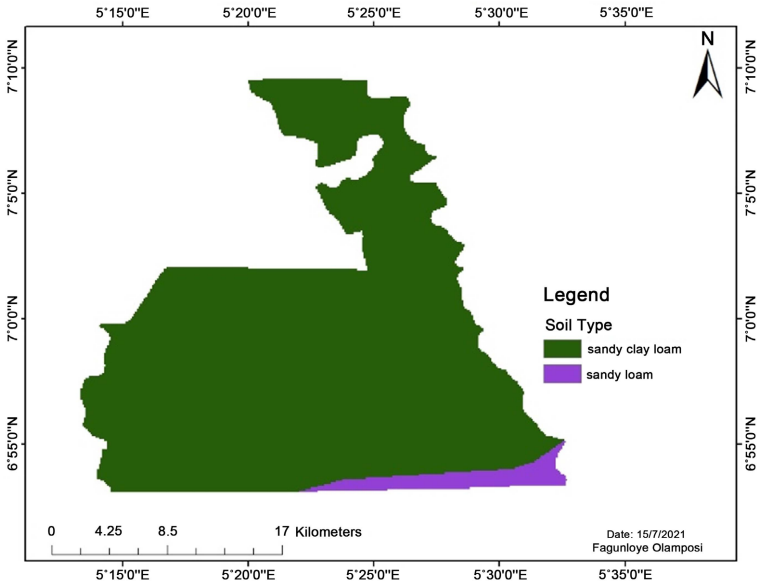


**Figure 8.** Soil map.

was then determined which of the created rainfall types had the greatest impact on flooding. Regions with higher yearly rainfall averages are thought to be more vulnerable to floods than areas with lower annual rainfall averages. Places with a lot of rain received a ranking of "5", while areas with little rain received a ranking of "1" (see Figure 9).

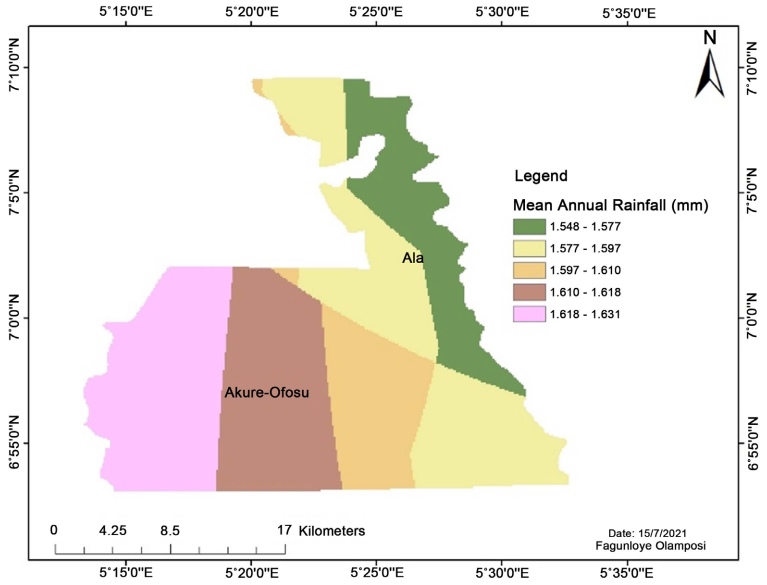


Figure 9. Spatial rainfall distribution map.

### 4.2.6. Flood Vulnerability Zones Based on Drainage Density

Noting that the structure and features of soil and rock affect drainage systems is essential. When there is a great deal of drainage in a limited region, leading to its susceptibility to erosion, there is massive sedimentation. As long as there are stream channels in the watershed, the density should be at least 5 or more. Both moderately and poorly drained zones have densities between 1 and 5, respectively. The research region contains streams of the first, second, and third order. In this study, areas with poor drainage obtained the highest ranks, while those with adequate drainage received the lowest.

Figure 13 shows the dendritic drainage pattern of second and third-stream orders. Nevertheless, the impact of river drainage on flood risk is governed by the geology and soil type, rainfall quantity, and evapotranspiration rates, among others. Analysis of drainage density revealed that the places most in danger of floods were not situated along river lines, but rather within the country's perimeter. As a result, the rivers go through places with high infiltration rates and good drainage.

Using the 30 m DEM, we can see that the research area's elevation spans from 49 meters to 426 meters above sea level. The highest elevation areas of the image are shown in gray (Figure 10). The area's stream network and Euclidean River Distance were generated using DEM. When water runs down a slope, the Euclidean River Distance map (Figure 11) reveals which cells are most likely to be impacted and collected by the water. To define the Flow accumulation, cells with the

highest values are located at the lowest points (Figure 12). The water will flow in the direction of the highest values.

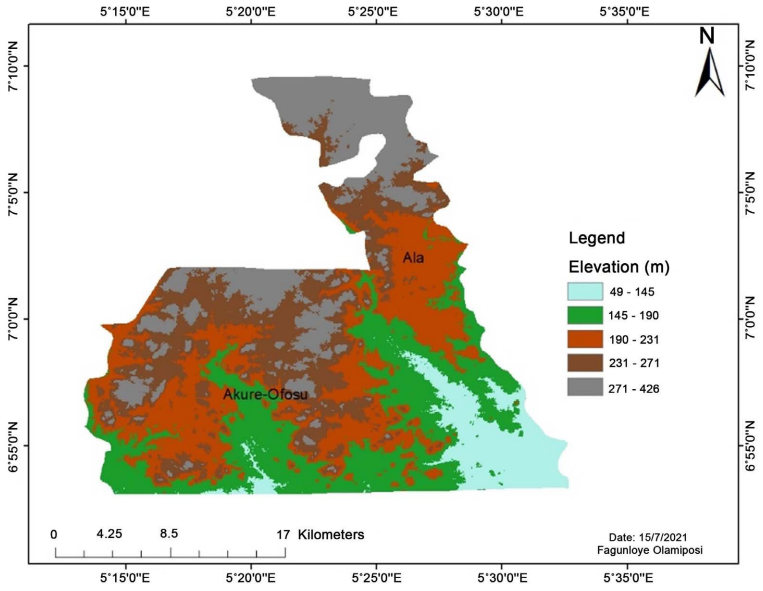


Figure 10. Elevation map.

Figure 13 is the stream network extracted from the SRTM. Also, Flow accumulation (Figure 12) and Euclidean River Distance (Figure 11) of the study area respectively. The different colors represent the different flow accumulation (and also the Distance to the River in Figure 11). As stated before, flow accumulations between 121,388 – 157,127 = very high; 70,861 – 121,388 = high; 28,961 – 70,861 = moderate; 5546 – 28,961 = low; and 0 – 5546 = very low rankings, respectively.

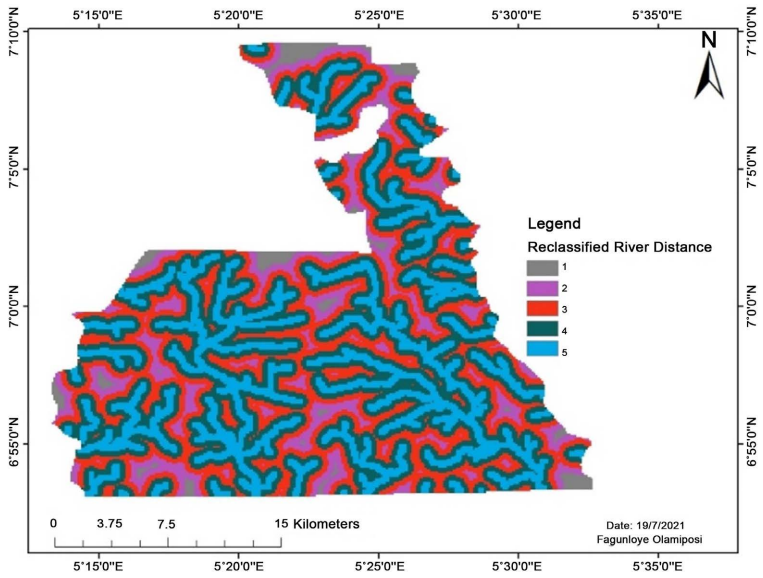


Figure 11. Euclidean River Distance map.

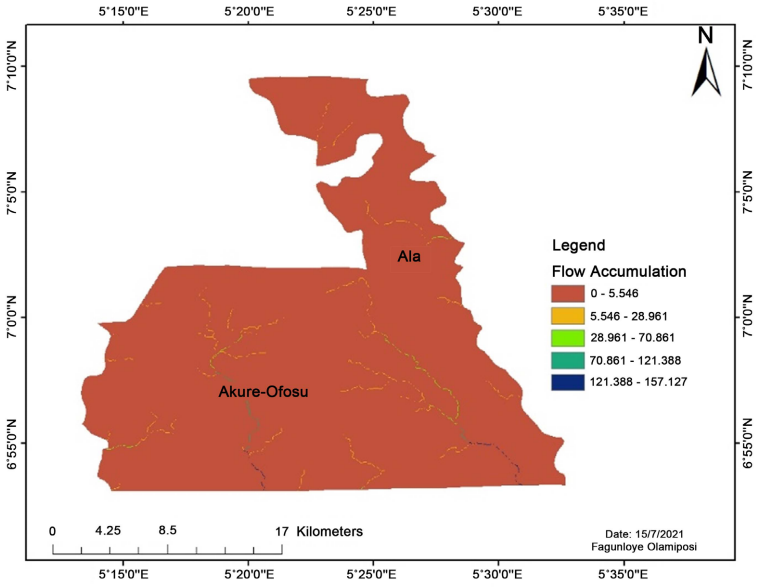


**Figure 12.** Flow accumulation map.

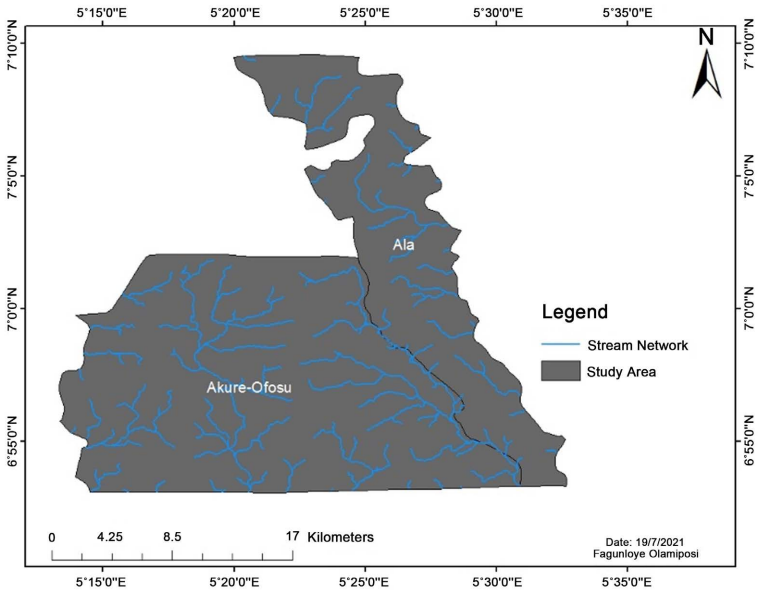


**Figure 13.** The stream network map.

Field investigations in the study area revealed that the once densely forested area has experienced massive deforestation in the last two decades, as well as the construction of buildings and the conversion of forests to farmlands, thereby increasing the rate of flooding. Additionally, high rainfall increases the runoff due to the expansion of the well-known "Ala River." Existing drainage systems are characterized by insufficiently sized culverts that are often clogged by waste deposition and silt buildup due to years of neglect and lack of maintenance. Due to growing residential, commercial, and infrastructural development, there is an increase in impermeable surfaces, and increasing stormwater runoff, according

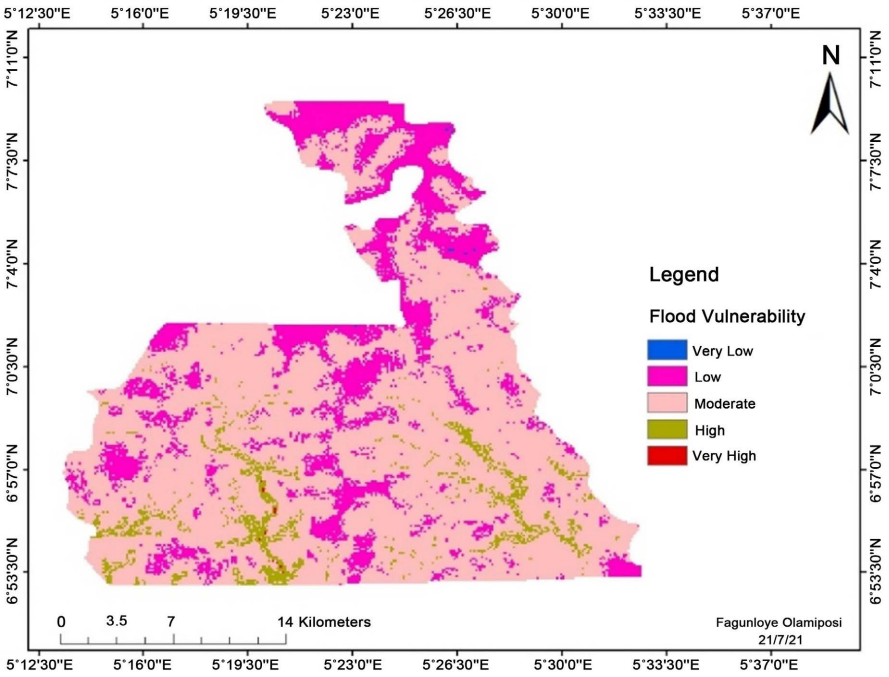


Figure 14. Flood vulnerability zone map.

to the findings of the investigation. It was also found that the restriction of natural stream flows by structures and the limited capacity of culverts and stream channels contribute to flooding.

The flood risk map which resulted from the multi-criteria analysis is shown in Figure 14 shows the field collection point of the area flooded (Table 3).

Table 3. The flood vulnerability statistics.

| Zone | Area Covered in Km$^2$ | Percentage |
|---|---|---|
| Very low | 0.1497 | 0.03 |
| Low | 122.69 | 21.23 |
| Moderate | 428.23 | 74.10 |
| High | 26.64 | 4.61 |
| Very high | 0.1797 | 0.03 |
| **Sum** | **577.8894** | **100** |

### 4.2.7. GIS Weighted Overlay Analysis

Combining the various theme levels yielded the regions in danger of flooding. Using the Spatial Analyst tool in ArcGIS, this research used the weighted overlay approach. Each layer was assigned a rank, and equal weights were allotted. The result was a flood risk map with five risk zones: Very High, High, Moderate, Low, and Very Low (Figure 15). The map result reveals that the research region has a sizeable zone of low vulnerability that spans a large area. The high and moderate danger zones. In addition to the Ala river basin, the extremely high-risk zones are also located in the Ala river basin. Due to their closeness to the "Ala River,"

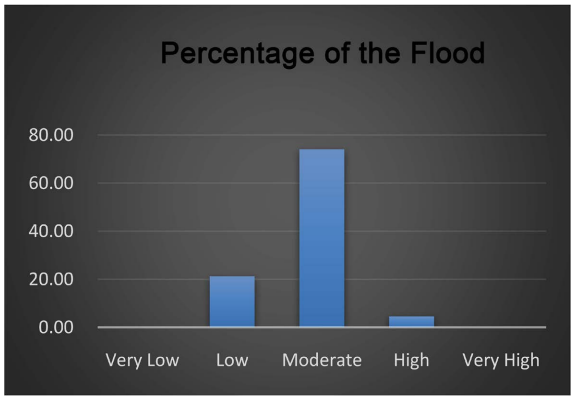


**Figure 15.** Chart of the flood risk zones.

they are also exposed to the possibility of floods. The majority of Built-up and Bare surface regions lie inside the High-risk zone.

As a result, regions of human habitation and activity such as townships, highways, rivers, and cultivated areas are taken into consideration in the risk map's depiction of risk and environmental formation. Land cover changes enhance a region's vulnerability to floods. Land cover maps, numbers, and percentage changes all play a role in various kinds of conversions and alterations. This includes a decline in the area's plant cover, which in turn increases surface runoff and the risk of flooding in low-lying regions where most settlements are situated.

### 4.3. SAR-Based Flooding Extent Mapping

The following images are what emerge after SAR images have been subjected to geometric rectification and binarization (**Figures 16-18**).

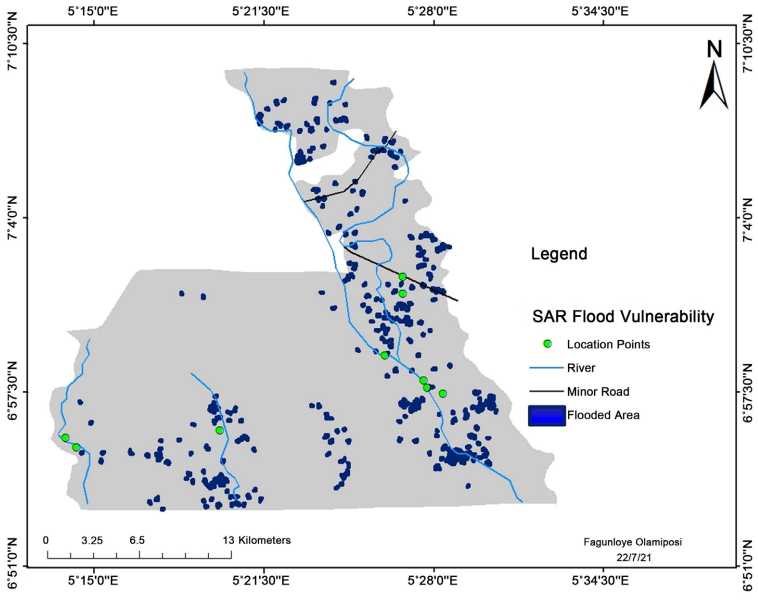


**Figure 16.** The flooded area on Radar image analysis.

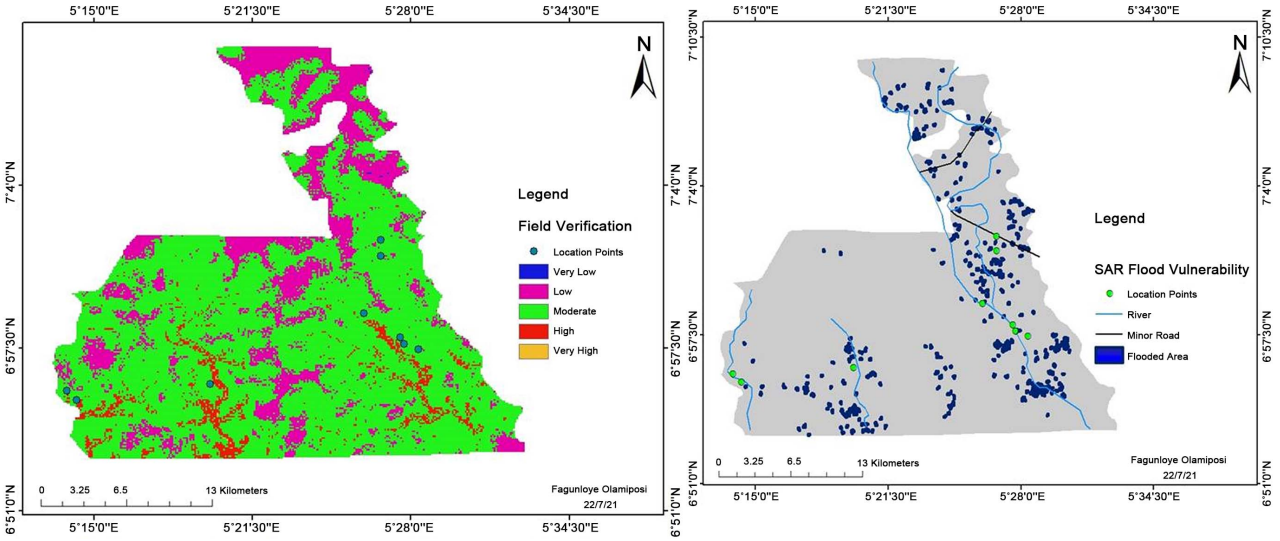


Figure 17. Image showing the comparison between the two results. Here, the result from MCA and the other from Radar image Analysis for the study area are placed side by side.

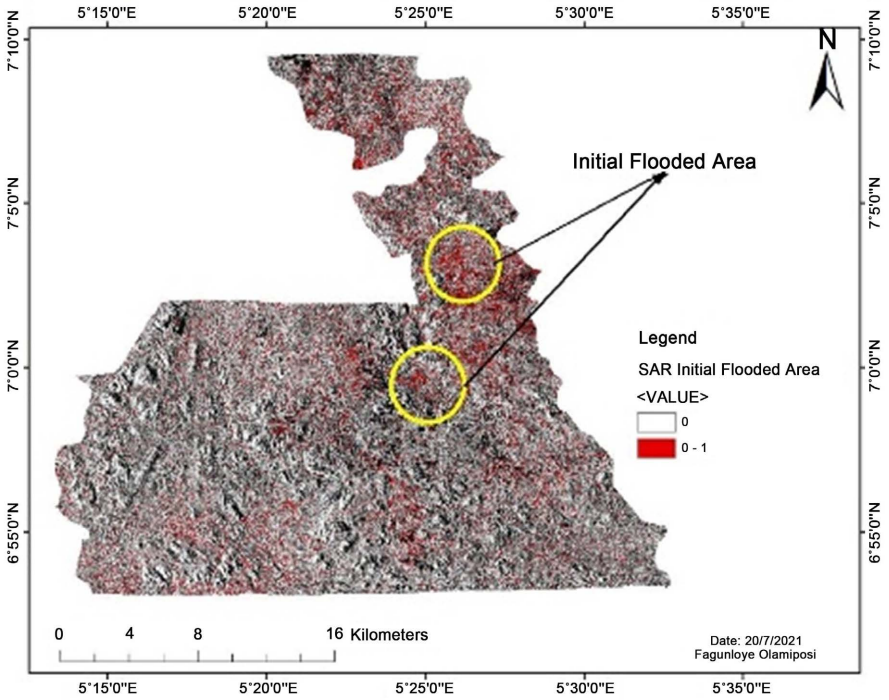


Figure 18. The flood area in red spotted through Radar image analysis.

The figure above (Figure 19) shows the affected areas on the Radar image flood extent map (see **Appendix A** for the process on Google Earth Engine). These are features that fall within the flooded area. They are depicted as red, which means danger. The features displayed here are farmlands, settlements, and camps. The farm's shapefile is the credit of Orbital Solutions. They mapped the reserves, and the data was collected from them.

The figure below (Figure 20) shows the affected areas on the MCA flood extent

map. These are features that fall within the flooded area. They are depicted as red, which means danger. The features displayed here are Farmlands, settlements, and camps. The farm's shapefile is the credit of Orbital Solutions. They mapped the reserves, and the data was collected from them.

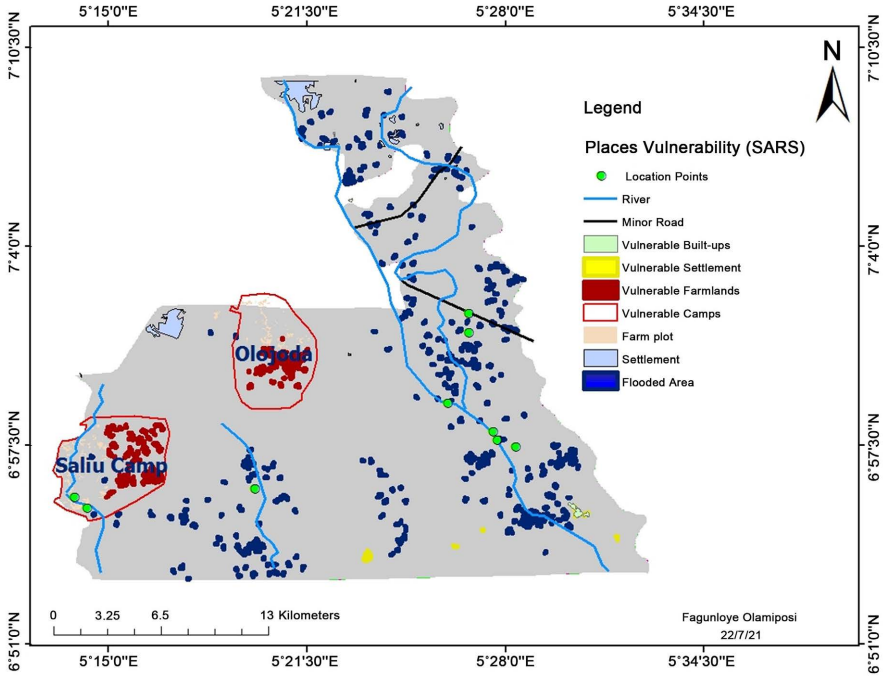


Figure 19. Map showing areas that fall into the flooded area extent on Radar image analysis result.

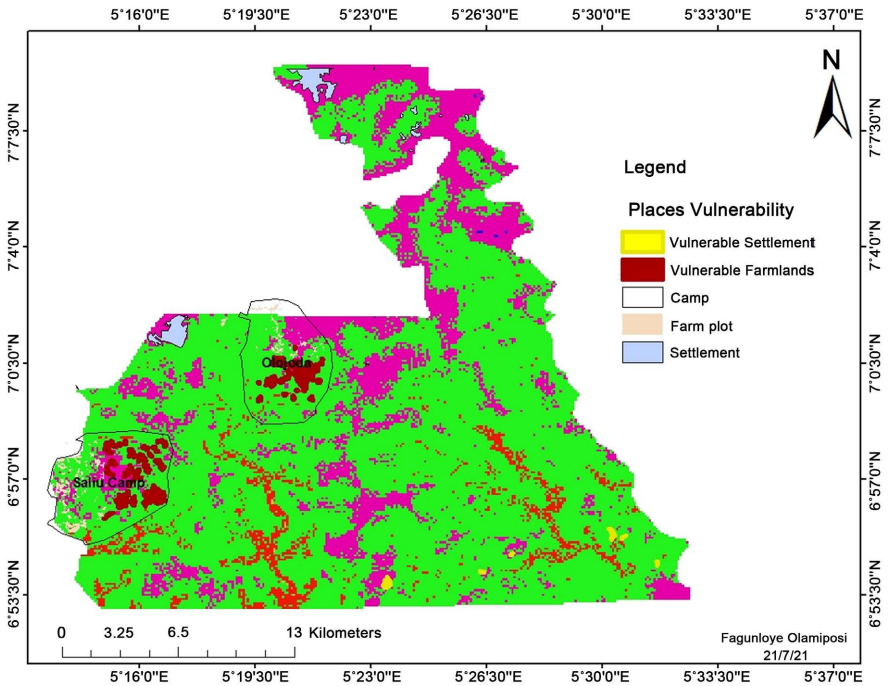


Figure 20. Map showing areas that fall into the flooded area extent on MCA result.

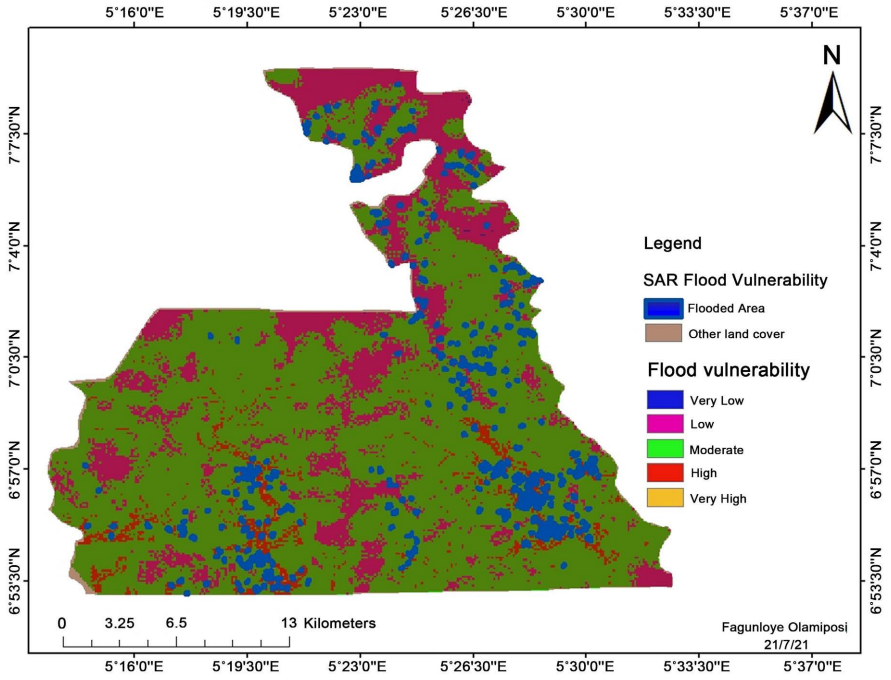


Figure 21. MCA and radar image analysis maps overlaid.

About 7% percent of the overall area is affected by flooding, while 74% is in the moderate risk zone while 21% is in the low-risk zone. According to the results of the research, the areas that are most likely to be inundated are those along the Ala River and those with a high spatial rainfall distribution.

The yellow and rose hues, which represent the high and moderate degrees of flooding from the multi-criteria analysis, correspond with the blue color, which represents the extracted water from the SAR imagery as shown in Figure 21. It is observed that the water level correlates to these two analyses but is more indicative of mild flooding. This might be due to several reasons, including the moisture and clay content of the diverse soil types and the lack of real-time satellite imagery of the flooding event. These factors need more investigation in the future.

## 5. Discussion

The goal of this study was to find flood-prone areas in the study area (Ala and Akure-Ofosu Communities) and make a GIS-based map of flood vulnerability. The focus was on the Ala River Basin and how urbanization and deforestation contributed to flooding. Sentinel 2A Image for the year 2020 was used to get a supervised classification image of the study area. Also, the surface hydrology and soil type were looked at to find out how much water infiltrated and seeped into the ground in different parts of the study area.

Land use and land cover map for 2020 satellite imagery were used, and spatial rainfall distribution soil map, flow direction, flow elevation, and slope were used to produce the flood vulnerability map that shows where floods are likely to

happen. Five of the most important types of land cover in the area were found in the Sentinel 2A image and extracted. They are waterbody, cropland, built-up area, forest cover, and rock outcrop. The forested area helps to lessen the effects of any kind of flooding by reducing surface runoff and often aids the infiltration of water. Floods have lessened in frequency and severity throughout time but at the loss of agricultural land and human settlements. Using this information, the accuracy of the categorized images was evaluated.

Several variables went into the creation of the flood risk map. These included the distribution of rainfall, the Euclidean River Distance, flow accumulation, slope, soil type, LULC, and elevation. ArcMap was used to reclassify the data, and then a pair-wise comparison was performed to determine the source of the flooding in the study region and its severity. Overlaying the reclassified layers was accomplished using a GIS-weighted overlay.

There was a total of 21% of the entire area covered by low-risk zones, 5% of the total area covered by high risk, and 74% of the total area covered by intermediate-risk zones.

Finally, Radar images of pre and post-flood events were computed using JavaScript on GEE to ascertain the level of flooding in the area in which 35.9 $km^2$ was flooded out of the 577.19 $km^2$ of the total area, which is about 6% of the total area were flooded. The final results of the Radar were overlaid on the image created using MCA, to compare the outputs of the two results.

## 6. Conclusions

Mapping flood risk is a crucial component for applicable land use planning in floodplain regions. It also helps municipal planners and officials prioritize their efforts to mitigate or aid after a natural disaster. The primary objective of the flood risk mapping that was carried out for this thesis was to precisely outline the regions of the study area that were in danger of flooding. It is accomplished by using a technique of multi-criteria assessment that is based on overlay analysis conducted inside a GIS context.

The method of multi-criteria analysis that was used in the process of mapping flood-vulnerability zones needed the combination of the following specified decision criteria: elevation, slope, rainfall, flow accumulation, Euclidean River Distance, land cover, and soil geology. The approach included the use of a variety of GIS operations as well as image processing procedures. In addition, the map that was produced reveals that more than seven percent of the region that was investigated is likely to be subjected to severe flooding.

In addition, SAR data was utilized to map the extent of the flooding by comparing data collected before and after the flooding event. The findings indicate that the SAR data obtained both before and shortly after the rainy season may be compared with the result obtained from the MCA. The high-risk locations that were highlighted by the MCA map correspond extremely well with the flooding extent map that was generated using the near real-time SAR data.

The MCA map indicates the expected level of flood hazard, but the radar analysis method is much more effective when there is access to real-time satellite imagery. The radar analysis map shows the areas that are covered with flood waters, while the MCA map indicates the expected level of flood hazard. The map that is produced as a result of the MCA analysis can serve as a guide for decision-makers and city planners, allowing for improved land use planning and flood risk management. On the other hand, radar analysis is most useful for managing disasters and directing relief measures, as it reveals precisely where flooding has taken place.

The approaches given in the study are relevant to other locations susceptible to flooding. Using high-resolution DEM data such as LIDAR, which will generate a flood inundation map with high accuracy and extensive rainfall data for accurate flood prediction analysis, or using UAV for generating DEM and Land Cover Map for the area can further improve the accuracy and visualization of the MCA work presented.

A future study might analyze other land cover categories and other factors (which are not covered in this study) that were inundated by superimposing the SAR-derived flood extent map with the land-use/cover categorization from Sentinel 2A data. It is advised to carry out a periodic investigation, real-time monitoring of flood susceptibility, early warning, and rapid damage assessment for the prevention of flood dangers and other environmental concerns.

A review of current literature reveals instances in which national or even regional flood risk maps have been created. The flood risk mapping approach has many benefits, including its user-friendliness, low cost, and simplicity with which maps are made public.

## Author's Contributions

O.F., acknowledges complete responsibility for study conceptualization and design, data collection, analysis and interpretation of results, and preparation of the manuscript. The author has read and agreed to the published version of the manuscript.

## Data Availability Statement

The SAR data in this study is publicly available on the Google earth engine platform, anyone can access data using their login ID and passwords. The data used are public and available to use, interested readers should check **Table 1** of this paper for the data sources used.

## Acknowledgements

First, I want to thank God Almighty for his unwavering devotion throughout my academic career.

My profound gratitude is also extended to my parents, Late Dr. and Mrs. Fagunloye, for their unwavering support. I would also like to thank my advisors,

Professor A.Y.B. Anifowose and Dr. Olabanji Aladejana for their participation and direction in completing this project.

Special thanks to my brother, Adeola Fagunloye, the academic and technical employees of the Department of Remote Sensing and GIS, as well as my friends and colleagues, who helped in many ways with work and encouraged me.

## Conflicts of Interest

The author declares no conflict of interest.

## References

[1] Jeb, D. and Aggarwal, S.P. (2008) Flood Inundation Hazard Modeling of the River Kaduna Using Remote Sensing and Geographic Information Systems. *Journal of Applied Sciences Research*, **4**, 822-1833.

[2] Herath, S. and Wang, Y. (2009) Case Studies and National Experiences. In: Sassa, K. and Canuti, P., Eds., *Landslides—Disaster Risk Reduction*, Springer, 475-497. https://doi.org/10.1007/978-3-540-69970-5_25

[3] James, L.D. and Hall, B. (1986) Risk Information for Floodplain Management. *Journal of Water Resources Planning and Management*, **112**, 485-499. https://doi.org/10.1061/(asce)0733-9496(1986)112:4(485)

[4] Granger, K.G., Jones, T., Leiba, M. and Greg, S. (1999) Community Risk in Cairns: A Multi-Hazard Risk Assessment. *Australian Journal of Emergency Management*, **14**, 25-26.

[5] Panayotis, P., Kortenhaus, A., SwerpeL, B. and Jiménez, J.A. (2008) Review of Flood Hazard Mapping. Flood Site Consortium, Spain.

[6] Mishra, K. (2013) Geomorphological Studies and Flood Risk Assessment of Kosi River Basin Using Remote Sensing and GIS Technique. Indian Institute of Remote Sensing, Indian Space Organization.

[7] Alliance Development Works and United Nations University (2014) World Risk Report; Focus; The City as a Risk Area. Bündnis Entwicklung Hilft and UNU-EHS.

[8] Intergovernmental Panel on Climate Change (IPCC) (2012) Managing the Risks of Extreme Events and Disasters to Advance Climate Change Adaptation. Cambridge University Press.

[9] World Meteorological Organization (2021) Weather-Related Disasters Increase over Past 50 Years, Causing More Damage but Fewer Deaths. https://wmo.int/media/news/weather-related-disasters-increase-over-past-50-years-causing-more-damage-fewer-deaths

[10] UNISDR (United Nations International Strategy for Disaster Reduction) (2009) Global Assessment Report on Disaster Risk Reduction. Technical Report.

[11] Adegbola, A.A. (2012) Historical Rainfall-Runoff Modeling of River Ogunpa, Ibadan, Nigeria. *Indian Journal of Science and Technology*, **5**, 2725-2728. https://doi.org/10.17485/ijst/2012/v5i5.5

[12] Agbola, B.S., Ajayi, O., Taiwo, O.J. and Wahab, B.W. (2012) The August 2011 Flood in Ibadan, Nigeria: Anthropogenic Causes and Consequences. *International Journal of Disaster Risk Science*, **3**, 207-217. https://doi.org/10.1007/s13753-012-0021-3

[13] Lillesand, T.M., Kiefer, R.W. and Chipman, J.W. (2008) Remote Sensing and Image Interpretation: 6th Edition. John Wiley & Sons.

[14] Wikipedia Contributors (2021) Köppen Climate Classification. Wikipedia. https://en.wikipedia.org/w/index.php?title=K%C3%B6ppen_climate_classification&oldid=1107119001

[15] Ayeni, A.O., Balogun, I.I. and Soneye, A.S.O. (2011) Seasonal Assessment of Physico-Chemical Concentration of Polluted Urban River: A Case of Ala River in Southwestern-Nigeria. *Research Journal of Environmental Sciences*, **5**, 22-35. https://doi.org/10.3923/rjes.2011.22.35

[16] Rahaman, M.A. (1988) Recent Advances in the Study of the Basement Complex of Nigeria. Precambrian Geology of Nigeria, Geological Survey of Nigeria, Kaduna South, 11-43.

[17] Oyawoye, M.O. (1970) The Basement Complex of Nigeria. In: Dessauragie, T.F.J. and Whiteman, Eds., *African Geology*, Ibadan University Press, 67-78.

[18] Jones, H.A. and Hockey, R.D. (1964) The Geology of Part of Southwestern Nigeria Geol. *Geological Survey of Nigeria Bulletin*, **31**, 1-101.

[19] Papaioannou, G., Vasiliades, L. and Loukas, A. (2014) Multi-Criteria Analysis Framework for Potential Flood Prone Areas Mapping. *Water Resources Management*, **29**, 399-418. https://doi.org/10.1007/s11269-014-0817-6

[20] Stefanidis, S. and Stathis, D. (2013) Assessment of Flood Hazard Based on Natural and Anthropogenic Factors Using Analytic Hierarchy Process (AHP). *Natural Hazards*, **68**, 569-585. https://doi.org/10.1007/s11069-013-0639-5

[21] Wikipedia Contributors (2021) Cohen's Kappa. Wikipedia. https://en.wikipedia.org/w/index.php?title=Cohen%27s_kappa&oldid=1105990419

[22] Ouma, Y. and Tateishi, R. (2014) Urban Flood Vulnerability and Risk Mapping Using Integrated Multi-Parametric AHP and GIS: Methodological Overview and Case Study Assessment. *Water*, **6**, 1515-1545. https://doi.org/10.3390/w6061515

## Appendix A

```
var before_start = '2020-03-15'
var before_end = '2020-07-30'
var after_start = '2020-07-30'
var after_end = '2020-08-30'

var geometry = (Ondo);
// Map.centerObject(geometry, 10);
Map.addLayer(geometry, {color: 'grey'}, 'Ondo State');

var collection    = ee.ImageCollection("COPERNICUS/S1_GRD")
        .filter(ee.Filter.eq("instrumentMode", "IW"))
        .filter(ee.Filter.listContains("transmitterReceiverPolarisation", "VH"))
        .filter(ee.Filter.listContains("transmitterReceiverPolarisation", "VV"))
        .filter(ee.Filter.eq("orbitProperties_pass", "ASCENDING"))
        .filter(ee.Filter.eq("resolution_meters", 10))
        .filterBounds(geometry)
        .select(['VV', 'VH']);

var beforeCollection = collection.filterDate(before_start, before_end)
var afterCollection = collection.filterDate(after_start, after_end)

var before = beforeCollection.mosaic().clip(geometry);
var after = afterCollection.mosaic().clip(geometry);

var addRatioBand = function(image){
   var ratioBand = image.select('VV').divide(image.select('VH')).ren
ame('VV/VH')
   return image.addBands(ratioBand)
}

var beforeRgb = addRatioBand(before)
var afterRgb = addRatioBand(after)
print(beforeRgb);

var visParams = {
   min: [-25,-25,0],
   max: [0,0,2]
}
Map.addLayer(beforeRgb, visParams, 'Before')
Map.addLayer(afterRgb, visParams, 'After')

Export.image.toDrive({
```

```
    image: after,
    description: "after_SAR",
    region: Ondo,
    scale: 10
});
// print(filtered.first());
```